6th European Conference on Computational Mechanics (ECCM 6)
7th European Conference on Computational Fluid Dynamics (ECFD 7)
1115 June 2018, Glasgow, UK

VISCOELASTIC-VISCOPLASTIC CONSTITUTIVE MODEL FOR UNIDIRECTIONAL FIBRE REINFORCED POLYMERS

P.-W. GERBAUD [1,2], F. OTERO[2,3], P. BUSSETTA[2], P. P. CAMANHO [2,4]

[1] ENS Cachan, Université Paris-Saclay, Av. du Président Wilson 61, Cachan 94235, France
pgerbaud@ens-paris-saclay.fr

[2] INEGI, Rua Dr. Roberto Frias, Porto 4200-465, Portugal
pwgerbaud@inegi.up.pt ; fotero@inegi.up.pt ; pbussetta@inegi.up.pt

[3] CIMNE, Centre Internacional de Metodes Numerics en Enginyeria, Gran Capita s/n
08034, Barcelona, Spain
fotero@cimne.upc.edu

[4] DEMec, Faculdade de Engenharia, Universidade do Porto
Rua Dr. Roberto Frias, Porto 4200-465,Portugal
pcamanho@fe.up.pt

Key words: Constitutive model, Fibre reinforced polymers, Viscoplasticity, Viscoelasticity, Invariant theory

Abstract. Composite materials are increasingly being introduced in automotive (e.g. BMW i-project) and aeronautical (e.g. Airbus A350 and Boeing 787) applications. These applications are exposed to loading conditions with various energies which result in a complex mechanical response, that is vital to accurately predict. In this work, a constitutive model which takes into account the viscous effects in the mechanical behaviour of a unidirectional carbon-epoxy system is presented. This model at the ply scale is based on the very efficient transversely isotropic elastic-plastic model proposed by Vogler et al. (*Modeling the inelastic deformation and fracture of polymer composites-Part I: Plasticity model*), which can be calibrated for other fibre reinforced polymers (FRPs). An excellent correlation between the measured and numerically predicted stress-strain responses of the specimens was achieved for all specimen types and both strain rate regimes.

1 INTRODUCTION

The number of applications in which FRPs are used in aeronautical and automotive structures is increasing quickly, and along with it comes the need to efficiently and precisely predict the behaviour of these structures under various loading scenarios. Composite structures may be subjected to high speed loading events and the numerical assessment of the dynamic material response is therefore relevant for several loading scenarios. Some examples are bird, tire and hail impact and crash events.

Strain rate effects and non-linear stress-strain behaviour must be captured by advanced composite material models to accurately predict the initiation and evolution of damage. It is therefore imperative to have appropriate material models.

The experimental data has been reported in [1] and [2] and describes the nonlinearities under multi-axial loadings prior to the onset of cracking. The necessary data to calibrate the presented model for the HexPly IM7-8552 material system is provided by these tests.

This work presents a new fully 3D transversely isotropic viscoelastic-viscoplastic constitutive model. The proposed model is implemented as a VUMAT (user material subroutine using an explicit formulation), in the Finite Element Analysis (FEA) commercial software package Abaqus. The available tension and compression tests are simulated using this VUMAT. By using the explicit capabilities of the Abaqus code, the strain-rate dependency of the global response is very accurately captured.

2 CONSTITUTIVE MODEL

2.1 Transversely isotropic formulation

The constitutive model originally proposed by Vogler et al. [3], and further developed by the authors is presented in this section. It represents a viscous extension to the original elastic-plastic model. The small deformation theory is used to formulate the equations of the model. Therefore, the following strain additive decomposition is assumed

$$\boldsymbol{\varepsilon} = \boldsymbol{\varepsilon}_{\text{ve}} + \boldsymbol{\varepsilon}_{\text{vp}}. \tag{1}$$

where -ve- stands for “viscoelastic” and -vp- for “viscoplastic”, while $\boldsymbol{\varepsilon}$ represents the total strains.

The use of structural tensors enables a formulation of the anisotropy free of any reference coordinate system. Therefore, the material symmetries are viewed as an intrinsic material property. The structural tensors constitute then an additional argument in the constitutive equations. Finally, finite fibre rotations can be regarded easily thanks to this formulation. The structural tensor $\boldsymbol{A}$ that represents the symmetry conditions of transversely isotropic materials is defined by the dyadic product of the unit vector of the preferred (fibre) direction $\underline{a}$

$$\boldsymbol{A} = \underline{a} \otimes \underline{a}. \tag{2}$$

Following the previous work reported in [3], the structural tensor is used as an additional argument in order to formulate the elastic free energy density, the yield function and the plastic potential formulation. In the proposed viscoelastic-viscoplastic extension, $\boldsymbol{A}$ is used in the formulation of the viscoplastic creep function, the viscoplastic potential and the viscoelastic model. The elastic free energy density for the proposed transversely isotropic model reads

$$\begin{aligned} \Psi(\boldsymbol{\varepsilon}, \boldsymbol{A}) \coloneqq & \frac{1}{2}\lambda(\text{tr}\boldsymbol{\varepsilon})^2 + \mu_T(\text{tr}\boldsymbol{\varepsilon})^2 + \alpha(\underline{a}\boldsymbol{\varepsilon}\underline{a})\text{tr}\boldsymbol{\varepsilon} \\ & + 2(\mu_L - \mu_T)(\underline{a}\boldsymbol{\varepsilon}^2\underline{a}) + \frac{1}{2}\beta(\underline{a}\boldsymbol{\varepsilon}\underline{a})^2, \end{aligned} \tag{3}$$

with the five elasticity constants λ, μ_T, μ_L, α, β as invariant coefficients.

The stress tensor $\boldsymbol{\sigma}$ and the elasticity tensor $\mathbb{C}_e$ can be obtained by computing the first and the second derivatives of the free energy density with respect to the strain tensor, respectively

$$\boldsymbol{\sigma} = \partial_{\boldsymbol{\varepsilon}} \Psi(\boldsymbol{\varepsilon}, \boldsymbol{A}) \quad , \quad \mathbb{C}_e = \partial^2_{\boldsymbol{\varepsilon}\boldsymbol{\varepsilon}} \Psi(\boldsymbol{\varepsilon}, \boldsymbol{A}). \tag{4}$$

In the model formulation, a decomposition of the stress tensor is done. The stress tensor is decomposed in three contributions as follows

$$\boldsymbol{\sigma} = \boldsymbol{s} + p\boldsymbol{I} + \sigma_f \boldsymbol{A}, \tag{5}$$

where $\boldsymbol{s}$ is the deviatoric part of the stress in the matrix, the $p\boldsymbol{I}$ term corresponds to the hydrostatic pressure in the matrix material component and the $\sigma_f \boldsymbol{A}$ term corresponds to the stress projected in the fibre direction (fibre contribution). The scalars p and σ_f are determined by imposing the following conditions

$$\boldsymbol{s} : \boldsymbol{I} = 0 \quad \text{and} \quad \boldsymbol{s} : \boldsymbol{A} = 0. \tag{6}$$

These conditions correspond to a trace of the deviatoric part equal to zero and no contribution of the fibre direction. They lead to the expression of p and σ_f

$$\begin{aligned} p &= \frac{1}{2}(\boldsymbol{\sigma} : \boldsymbol{I} - \boldsymbol{\sigma} : \boldsymbol{A}), \\ \sigma_f &= \frac{1}{2}(3\,\boldsymbol{\sigma} : \boldsymbol{A} - \boldsymbol{\sigma} : \boldsymbol{I}). \end{aligned} \tag{7}$$

This decomposition will be used for the viscoplastic and viscoelastic formulation.

2.2 Viscoplastic formulation

Similarly to the plastic formulation, a decomposition of the stress state in "viscoplasticity inducing" stresses and assumed "elastic reaction" stresses is used. The 'viscoplasticity inducing" part of the stresses has an influence on the viscoplastic behaviour (yield and plastic evolution), and it is used further in the formulation of the plastic yield function. On the other side, the "elastic reaction" part of the stresses plays no role in the plasticity (e.g. hydrostatic pressure in the polymeric matrix).

$$\boldsymbol{\sigma} = \boldsymbol{\sigma}_{\text{e,reac}} + \boldsymbol{\sigma}_{\text{vp,ind}}, \tag{8}$$

where the "elastic reaction" and "viscoplasticity inducing" stresses are defined using Eq. 9

$$\begin{aligned} \boldsymbol{\sigma}_{\text{e,reac}} &= p\boldsymbol{I} + \sigma_f \boldsymbol{A}, \\ \boldsymbol{\sigma}_{\text{vp,ind}} &= \boldsymbol{\sigma} - \boldsymbol{\sigma}_{\text{e,reac}} = \boldsymbol{s}. \end{aligned} \tag{9}$$

As can be seen, the elastic reaction stresses contain the hydrostatic pressure, and the stresses in the fibre direction which are both assumed purely elastic. Therefore, the "viscoplasticity inducing" stresses can be obtained directly from the total stresses using the fourth order tensor $\mathbb{P}_{\text{vp,ind}}$ according to

$$\boldsymbol{\sigma}_{\text{vp,ind}} \;=\; \mathbb{P}_{\text{vp,ind}} : \boldsymbol{\sigma}, \tag{10}$$

with

$$\mathbb{P}_{vp,ind} \;=\; \mathbb{I} - \frac{1}{2}\boldsymbol{I}\otimes\boldsymbol{I} - \frac{3}{2}\boldsymbol{A}\otimes\boldsymbol{A} + \frac{1}{2}(\boldsymbol{A}\otimes\boldsymbol{I} + \boldsymbol{I}\otimes\boldsymbol{A}). \tag{11}$$

In this expression, $\mathbb{I}$ is the fourth order unit tensor defined such that $I_{ijkl} = \delta_{ik}\delta jl$. The defined stresses are then used to formulate the viscoplastic creep surface using the invariant theory. The set of invariants that are used in the model are the following

$$\begin{aligned}
\mathrm{I}_1 &= \frac{1}{2}\,\mathrm{tr}(\boldsymbol{\sigma}_{\text{vp,ind}})^2 - \underline{a}\,(\boldsymbol{\sigma}_{\text{vp,ind}})^2\,\underline{a},\\
\mathrm{I}_2 &= \underline{a}\,(\boldsymbol{\sigma}_{\text{vp,ind}})^2\,\underline{a},\\
\mathrm{I}_3 &= \mathrm{tr}(\boldsymbol{\sigma}) \;-\; \underline{a}\,\boldsymbol{\sigma}_{\text{vp,ind}}\,\underline{a}.
\end{aligned} \tag{12}$$

The corresponding transversely isotropic viscoplastic surface reads

$$f(\boldsymbol{\sigma}, \dot{\boldsymbol{\varepsilon}}, \bar{\varepsilon}_{\text{vp}}, \boldsymbol{A}) = \alpha_1\mathrm{I}_1 + \alpha_2\mathrm{I}_2 + \alpha_3\mathrm{I}_3 + \alpha_{32}\mathrm{I}_3^2 - 1 \leq 0, \tag{13}$$

where

$$\begin{aligned}
&\alpha_3 = \alpha_3^t \quad \alpha_{32} = \alpha_{32}^t \quad \text{if} \quad \mathrm{I}_3 > 0,\\
&\alpha_3 = \alpha_3^c \quad \alpha_{32} = \alpha_{32}^c \quad \text{if} \quad \mathrm{I}_3 \leq 0.
\end{aligned} \tag{14}$$

The proposed viscoplastic creep function results in 6 viscoplastic creep parameters that have to be determined. Each of these parameters and the corresponding invariants are related to the following loading states: transverse shear, in-plane shear, uniaxial and biaxial transverse tension and uniaxial and biaxial transverse compression. Fig. 1 shows a schematic representation of the transversely isotropic f surface in the stress space. The points represented in the curves are the "trigger points" of the viscoplastic creep surface, for a given strain rate, in which the viscoplastic process is controlled. That is, in each of these points, an initial yield stress and a hardening curve giving the yield stress vs. the corresponding equivalent viscoplastic strain is defined via tabulated data. Consequently, the viscoplastic creep surface parameters $\alpha_{(\dots)}$ are a function not only of the strain rate [1], but also of the equivalent viscoplastic strain, see [3].

The evolution of the viscoplastic strain is defined by using a non-associative flow rule. Two viscous parameters define the Perzyna type over stress model, m, and η. The consistency parameter γ_{vp} is to be determined using the flow rule. The flow rule reads

$$\dot{\boldsymbol{\varepsilon}}_{\text{vp}} = \gamma_{\text{vp}}\boldsymbol{n}_{\text{g}} = \frac{\langle f(\boldsymbol{\sigma}, \dot{\boldsymbol{\varepsilon}}, \bar{\varepsilon}_{\text{vp}}, \boldsymbol{A})^m\rangle}{\eta}\boldsymbol{n}_{\text{g}}, \tag{15}$$

where $\mathrm{g}(\boldsymbol{\sigma}, \boldsymbol{A})$ is the function of the viscoplastic potential, which defined the non-associated viscoplastic flow direction $\boldsymbol{n}_{\text{g}} = \partial_{\boldsymbol{\sigma}}\mathrm{g}(\boldsymbol{\sigma}, \boldsymbol{A})$, analogous to plasticity. The crucial difference in the rate independent case is that now, stress states outside of the yield locus are admissible. That is, the stresses can exceed the yield surface depending on the loading velocity and are not

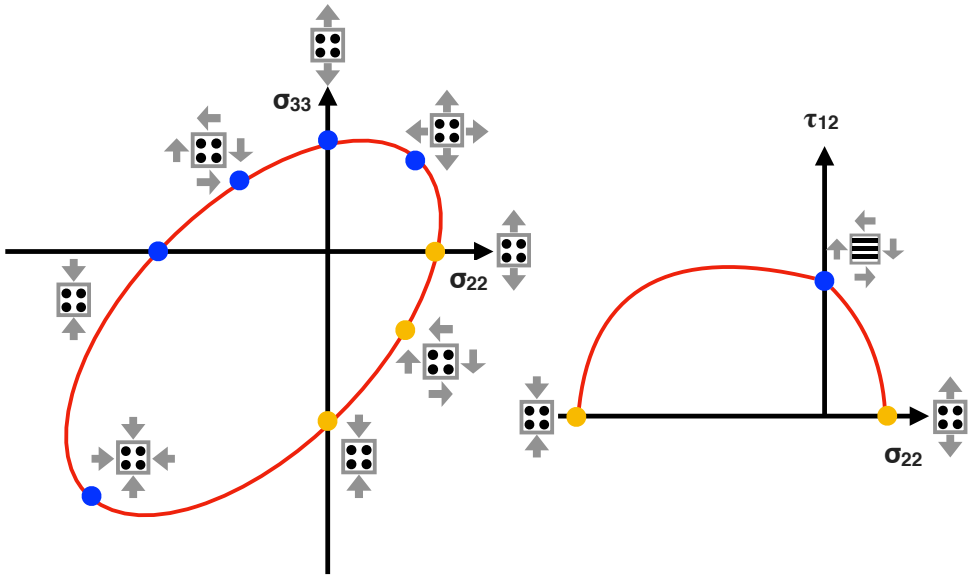

Figure 1: Schematic representation of the yield surface for UD composites in stress space (the yellow points are repetitions of the blue ones because of the material symmetry).

supposed to remain on the yield locus during plastic loading. The viscosity parameter acts as delay parameter. At $t = t_{n+1}$, the viscoplastic multiplier reads:

$$\gamma_{vp}^{n+1} = \frac{\langle f^m(\boldsymbol{\sigma}^{n+1}, \bar{\varepsilon}_{vp}^{n+1}, \mathbf{A})\rangle}{\eta} \Delta t^{n+1}, \tag{16}$$

with $\Delta t^{n+1} = t^{n+1} - t^n$. The consistency condition, which has to be fulfilled in the viscoelastic-viscoplastic case, reads

$$\gamma_{vp}^{n+1} \frac{\eta}{\Delta t^{n+1}} = \langle f^m(\boldsymbol{\sigma}^{n+1}(\gamma_{vp}^{n+1}))\rangle. \tag{17}$$

This consistency condition Eq. (17) can be solved with the Newton-Raphson method to obtain the value of the consistency parameter γ_{vp}^{n+1}. Then, the $\boldsymbol{\varepsilon}_{vp}^{n+1}$ can be updated at the end of the current time step.

2.3 Viscoelastic formulation

The viscoelastic extension implemented is based on the model proposed by Kaliske in [4]. It derives from a generalised Maxwell model as can be seen on Fig. 2. In this model, there is one main branch made of one linear spring, the elastic modulus is C_0 (the index of the branch is 0), which is the original elastic modulus of the material (quasi-static property). There is another branch in parallel. It is constituted of one Maxwell element, characterised by its elastic modulus C_1 and its relaxation time τ_1 (the index of that branch is 1). The equations for the 1-dimension rheological model are presented, before their generalisation for the fully 3D model. The total stress in the viscoelastic branch can be decomposed

$$\sigma = \sigma_0 + \sigma_1, \tag{18}$$

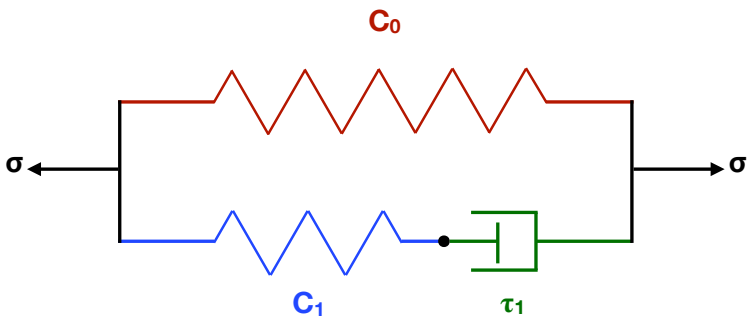

Figure 2: Schematic representation of the generalized 1D viscoelastic Maxwell model.

The differential equation for the stress in the Maxwell element reads

$$\Gamma_1 \, \dot{\sigma_0} = \dot{\sigma_1} + \frac{1}{\tau_1} \, \sigma_1, \tag{19}$$

with $\Gamma_1 = C_1 C_0^{-1}$.
The analytical solution reads

$$\sigma_1(t) = \int_0^t \Gamma_1 \exp\Big(- \frac{t - t^*}{\tau_1} \Big) \, \frac{\partial \sigma_0}{\partial t^*} \, dt^*. \tag{20}$$

In a reccurency scheme, at $t = t_{n+1}$ and by assuming a linear evolution of the stress σ_0 between t_{n+1} and t_n ($\Delta t^{n+1} = t^{n+1} - t^n$), an approximation of the solution can be obtained

$$\sigma_1^{n+1} \approx \exp(-\Delta t^{n+1}/\tau_1)\sigma_1^n + \Gamma_1 \, \frac{1 - \exp(-\Delta t^{n+1}/\tau_1)}{\Delta t^{n+1}/\tau_1} \, (\sigma_0^{n+1} - \sigma_0^n). \tag{21}$$

For the next sections, in order to simplify the expressions, the following notation are adopted, for the step $n+1$

$$f_1^{n+1} = \exp(-\Delta t^{n+1}/\tau_1), \quad \text{and} \quad f_2^{n+1} = \frac{1 - \exp(-\Delta t^{n+1}/\tau_1)}{\Delta t^{n+1}/\tau_1}. \tag{22}$$

Following Eq. 21, it is possible to fully determine the stresses at a given step using the previous stresses (which must be saved). Only the stress in the branch 1 depends on the strain rate.

The same equations can be implemented for the 3D scenario. However, fourth order tensors must be used instead of scalars ($\mathbb{C}_0, \mathbb{C}_1$, and $\mathbb{\Gamma}_1 = \mathbb{C}_1 : \mathbb{C}_0^{-1}$). The characteristic relaxation time tensor $\mathbb{T}_1$ is chosen such that

$$\mathbb{T}_1 = \tau_1 \mathbb{I}. \tag{23}$$

This choice simplifies the model formulation by using only one characteristic time parameter for every direction. More experimental data is necessary to determine the relaxation times in every direction. Poon and Ahmad have implemented in [5], a thorough relaxation time tensor successfully , using similar relaxation times.

Thefore, the system of equations is the following

$$\begin{aligned}
\boldsymbol{\sigma}_0^{n+1} &= \boldsymbol{\sigma}_0^n + \mathbb{C}_0 : \delta\boldsymbol{\varepsilon}_0^{n+1}, \\
\boldsymbol{\sigma}_1^{n+1} &= f_1^{n+1}\,\boldsymbol{\sigma}_1^n + f_2^{n+1}\,\mathbb{\Gamma}_1 : (\boldsymbol{\sigma}_0^{n+1} - \boldsymbol{\sigma}_0^n) = \boldsymbol{\sigma}_1^n + f_2^{n+1}\,\mathbb{\Gamma}_1 : \mathbb{C}_0 : \delta\boldsymbol{\varepsilon}_0^{n+1}, \\
\boldsymbol{\sigma}^{n+1} &= \boldsymbol{\sigma}_0^{n+1} + \boldsymbol{\sigma}_1^{n+1}.
\end{aligned} \tag{24}$$

The viscoelastic prediction is now expressed in term of the predicted stress $\boldsymbol{\sigma}^{pred,n+1}$ as

$$\boldsymbol{\sigma}^{pred,n+1} = \boldsymbol{\sigma}_0^n + f_1^{n+1}\boldsymbol{\sigma}_1^n + \mathbb{C}_{ve} : \delta\boldsymbol{\varepsilon}^{n+1}, \tag{25}$$

with

$$\mathbb{C}_{\text{ve}} = [\mathbb{I} + f_2^{n+1}\mathbb{\Gamma}_1] : \mathbb{C}_0. \tag{26}$$

The relaxation tensor $\mathbb{\Gamma}$ ($\hat{\mathbf{\Gamma}}$ using the Voigt notation) for a transverse isotropic material in the material coordinate system (1 is the direction of the fibres) is

$$\hat{\mathbf{\Gamma}} = \begin{bmatrix}
\gamma_{11} & \gamma_{12} & \gamma_{12} & 0 & 0 & 0 \\
\gamma_{21} & \gamma_{22} & \gamma_{23} & 0 & 0 & 0 \\
\gamma_{21} & \gamma_{23} & \gamma_{22} & 0 & 0 & 0 \\
0 & 0 & 0 & \gamma_{44} & 0 & 0 \\
0 & 0 & 0 & 0 & \gamma_{44} & 0 \\
0 & 0 & 0 & 0 & 0 & \gamma_{66}
\end{bmatrix}. \tag{27}$$

There are different methods to determine $\mathbb{\Gamma}$ in the correct coordinate system. One is to define the independent parameters (maximum 7) of this fourth order tensor in the material coordinate system, then transform it into a matrix form, rotate that matrix in the current coordinate system and finally rewrite it as a fourth order tensor. This approach is complicated because all the parameters must be calibrated and the rotation. Another approach might reduce the number of parameters. It consists in using one single scalar, $\gamma_{ve,1}$, which multiplies an order four tensor, $\mathbb{P}_{\text{ve,ind}}$. This tensor, defined using the preferred direction vector $\underline{a}$, is used to extract from the stress/strain, the components that have an influence on the viscoelastic behaviour (e.g. shear in the polymeric matrix), and remove the components which do not depend on the strain-rate (e.g. stress in the elastic fibre). Therefore, it must be checked afterwards that using only one parameter is accurate enough. Kaliske et al. have reported in [4] that the viscoelastic behaviour is in many cases mainly linked to the isochoric part of the deformation, which excludes the hydrostatic pressure contribution. In the presented model, the viscoelasticity is considered not linked to the hydrostatic pressure in the polymeric matrix and neither to the fibres, where the behaviour is assumed purely elastic. Consequently, the "viscoelasticity inducing" stresses is defined (part of the stress that depends on the strain rate in the viscoelastic response), which is exactly the same as the previously presented "viscoplasticity inducing" stresses (see Eq. 9).

$$\boldsymbol{\sigma}_{\text{ve,ind}} = \mathbb{P}_{\text{ve,ind}} : \boldsymbol{\sigma} = \mathbb{P}_{\text{vp,ind}} : \boldsymbol{\sigma}. \tag{28}$$

Therefore, $\mathbb{\Gamma}_1$ can be expressed using $\mathbb{P}_{\text{ve,ind}}$

$$\mathbb{\Gamma}_1 = \gamma_{\text{ve},1} \mathbb{P}_{\text{ve,ind}}. \tag{29}$$

This leads to the following expression of the viscoelastic stress $\boldsymbol{\sigma}_1^{n+1}$

$$\boldsymbol{\sigma}_1^{n+1} \;=\; f_1^{n+1}\, \boldsymbol{\sigma}_1^{n} + f_2^{n+1}\, \gamma_{\text{ve},1}\, \mathbb{P}_{\text{ve,ind}} : \mathbb{C}_0 : \delta\boldsymbol{\varepsilon}_{\text{ve}} \tag{30}$$

With this approach, the number of parameters for this model is reduced. Moreover, the model can easily be used for any orientation (using the preferred direction vector $\underline{a}$), as there is no need to transform a fourth order tensor. The viscoelastic extension is fully determined using only two scalar parameters, τ_1 and $\gamma_{\text{ve},1}$.

3 Calibration of the viscous parameters

It is assumed that the viscous behaviour is independent of the hydrostatic pressure. Hence, the strain rate dependency on the yielding behaviour and on the elastic behaviour is similar both in tension and in compression.

3.1 Calibration of the viscoplastic model parameters

The calibration of the two viscoplastic parameters, m and η, introduced in Eq. (15) is discussed herein. For the current material, IM7-8552, just two strain rate regimes were tested. Consequently, the parameter m is set to $m = 1$, and an approximately linear dependency of the viscoplastic yield stress on the logarithmic strain rate can be modelled using the parameter η. Although such a linear dependency from the logarithmic strain rate for carbon-epoxy is reported by [6], it cannot be assumed for arbitrary matrix materials. Thermoplastics for instance, or thermoplastic toughened resins, exhibit a nonlinear dependency on the logarithmic strain rate [7]. To account for this nonlinear dependency, the parameter m of the viscoplastic model can be used. Therefore, test data for at least 3 strain rate regimes are required to calibrate the parameter m.

To calibrate the remaining viscoplastic parameter η, the axial stress-strain curves of the 45° off-axis compression tests are used. These tests were performed at two different strain rates, at quasi-static rate (0.0004 s^{-1}) and at an axial strain rate of approximately 280 s^{-1}. The calibration is first performed by running a single element test and then a more refined test using a fine mesh, whereby the parameter $\eta = 4.0 \cdot 10^{-4}$ Ns/mm^2 gives the best approximation.

3.2 Calibration of the viscoelastic model parameters

The calibration of the two viscoelastic parameters $\gamma_{\text{ve},1}$ and τ_1 of the generalized Maxwell model, introduced in Eq. 23 and 29, is done performing the $90°$ compression tests. Indeed, under transverse solicitations, the response is rate-dependent and controlled by the matrix. Currently, it seems more obvious to calibrate the viscoelastic response caused by the matrix using this case. The $45°$ tests are used to control the validity of the model under shear solicitations but are less sensible to the value of $\gamma_{\text{ve},1}$ so they cannot be used independently. Approximated values are obtained using a 1D calculation, and then refined using a finite elements simulation

with a fine mesh, reproducing the experimental conditions. Only two strain-rate regimes are available, therefore a great uncertainty for the value of τ_1 exists. Indeed, no noticeable difference is observed for values in the range of 10^{-1} to 10^{-4} s. Therefore, τ_1 is set to $\tau_1 = 1 \cdot 10^{-2}$ s and the value $\gamma_{\text{ve},1} = 0.35$ is found for the best approximation.

4 Results

The simulated results are obtained using the (FEA) commercial software Abaqus. The experimental specimens are reproduced using three-dimensional, eight-node C3D8R solid elements with reduced integration. For low strain rates simulations, the viscoelasticity transforms into pure linear elasticity. Consequently, the element size effect on the results is very little. However, it is more important to refine the mesh under high strain rates because all areas in the specimen do not necessarily deform at the same speed. For these reasons, the following results have been obtained using a coarse mesh for the quasi-static simulations, and a very fine mesh for the dynamic simulations (hourglass effect was invesigated and not detected). The simulated cases are off-axis $15°$, $30°$, $45°$ and $90°$ transverse tension and off-axis $15°$, $30°$, $45°$, $60°$, $75°$ and $90°$ transverse compression.

On the following figures, the experimental and simulated axial strain-stress curves are plotted. They are obtained for dynamic and quasi-static regimes for both tension and compression. The dotted lines refer to the dynamic data, the continuous lines refer to the quasi-static data. Also, the red colour is used for the simulation results, while the black colour is used for the experimental results. Note that, the damage and the failure are not taken into account by the presented model.

4.1 Tension results

The Figs. 3 to 6 show the measured and simulated static and dynamic axial stress-strain curves under 15°, 30°, 45° off-axis tension and 90° transverse tension. Considering the experimental data of the dynamic tests, it can be seen that with a higher strain rate the initial slope increases. This means that viscous effects are observed in the elastic range and these must be taken into account. Here, the model is able to provide an excellent prediction of these effects. Also, the stress-strain curves become more linear under dynamic loading (See Figs. 3-6), according to the viscoplastic behaviour of the material which is modelled here. In that respect, the viscous effects noticed in both, elastic and plastic ranges, are very accurately predicted for the four orientations, validating the model for tensile loadings.

4.2 Compression results

The Figs. 7 to 12 show the measured and predicted axial stress-strain curves for 15°, 30°, 45°, 60°, 75° off-axis compression and 90° transverse compression under quasi-static and dynamic loadings. As can be observed, a very good prediction of the nonlinear behaviour has been achieved for both, quasi-static and dynamic loading cases. For compression loadings as well as

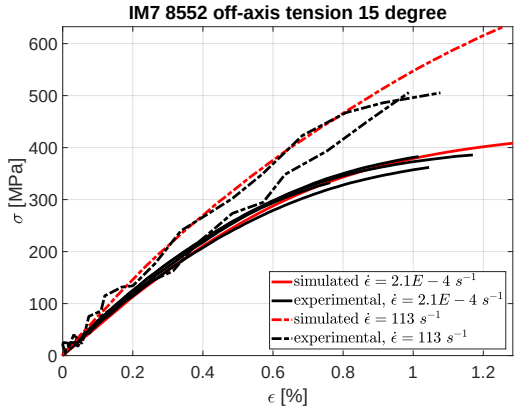

Figure 3: Axial stress-strain curves for the tensile tests and simulations, 15 degree, viscoelastic-viscoplastic model.

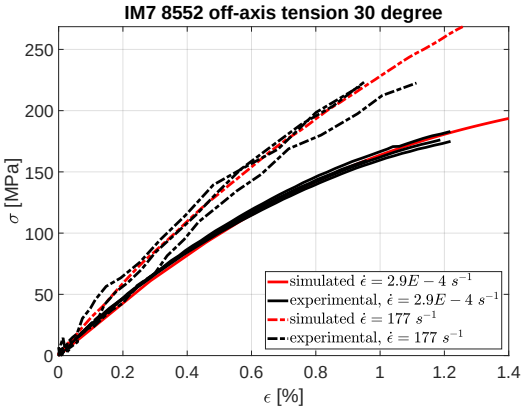

Figure 4: Axial stress-strain curves for the tensile tests and simulations, 30 degree, viscoelastic-viscoplastic model.

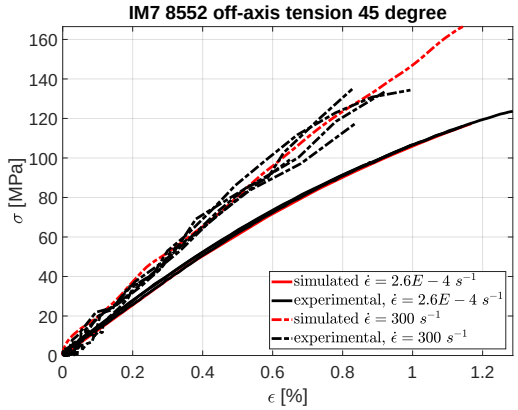

Figure 5: Axial stress-strain curves for the tensile tests and simulations, 45 degree, viscoelastic-viscoplastic model.

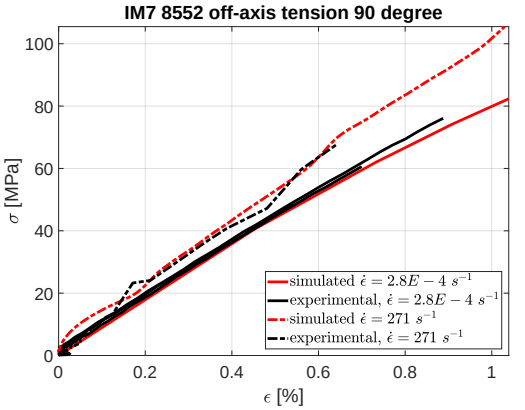

Figure 6: Axial stress-strain curves for the tensile tests and simulations, 90 degree, viscoelastic-viscoplastic model.

tensile loadings, the viscous effects are well taken into account by the presented model. Nevertheless, it is to be noted that for the 15°, 30°, 45° off-axis dynamic compression, the quadratic evolution in the plasticity domain cannot be reproduced completely using the presented model. A more thorough viscoplastic model, including the damage, could improve the predictions for those low angle specimens.

5 CONCLUSIONS

In this paper, a fully 3D viscoelastic-viscoplastic material model at the ply scale, is presented. It is currently written in a infinitesimal strain formulation and is implemented in a VUMAT for the (FEA) commercial software Abaqus. By using the preferred direction vector in the formulation, challenges with defining the proper orientation system are avoided. Consequently, the model can be used with any orientation. Due to the viscous extension, the prediction of the stresses state in a specimen is accurate for high strain rate regimes, which is very important

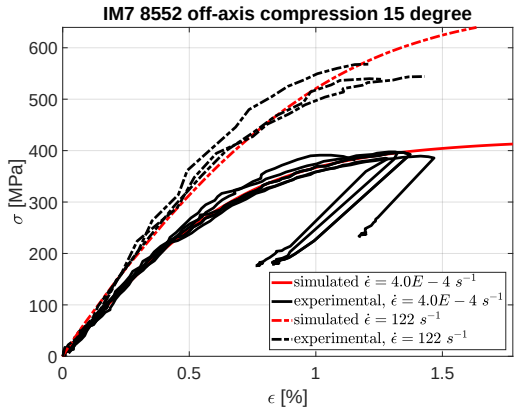

Figure 7: Axial stress-strain for the compression tests and simulations, 15 degree, viscoelastic-viscoplastic model.

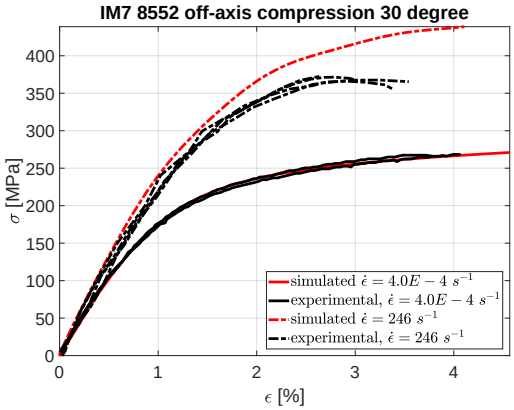

Figure 8: Axial stress-strain curves for the compression tests and simulations, 30 degree, viscoelastic-viscoplastic model.

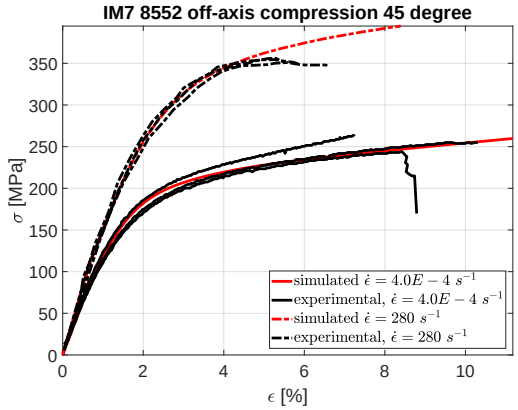

Figure 9: Axial stress-strain curves for the compression tests and simulations, 45 degree, viscoelastic-viscoplastic model.

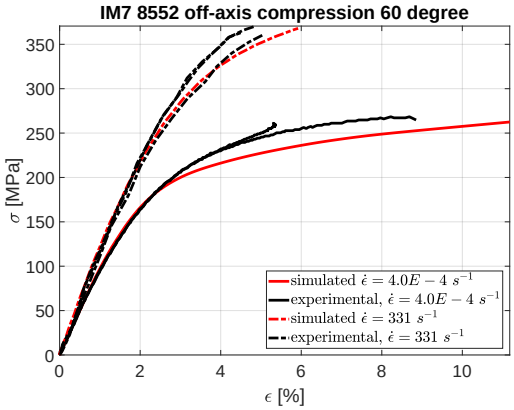

Figure 10: Axial stress-strain curves for the compression tests and simulations, 60 degree, viscoelastic-viscoplastic model.

for this field of research. Furthermore, its low number of viscous parameters makes it quick to calibrate. The model is able to predict nonlinearities under multi-axial loading conditions prior to the onset of cracking. The necessity to capture the viscous effects in the elastic range was also shown. Of further importance is the development of a strain rate dependent damage model taking into account the dynamic fracture toughnesses.

ACKNOWLEDGEMENTS

The second and third authors gratefully acknowledge the funding of Project NORTE-01-0145-FEDER-000022 SciTech Science and Technology for Competitive and Sustainable Industries, co-financed by Programa Operacional Regional do Norte (NORTE2020), through Fundo Europeu de Desenvolvimento Regional (FEDER).

The last author gratefully acknowledges the funding of Project PTDC/EMS-PRO/4732/2014, co-financed by Programa Operacional Competitividade e Internacionalização.

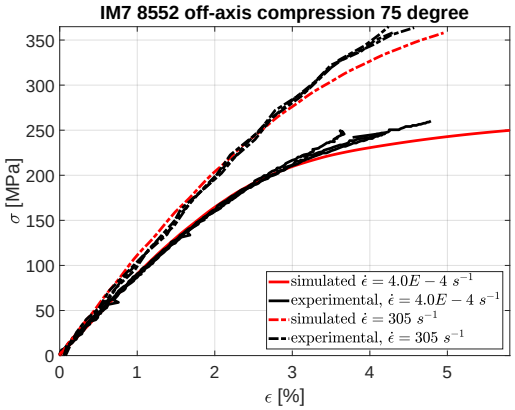

Figure 11: Axial stress-strain curves for the compression tests and simulations, 75 degree, viscoelastic-viscoplastic model.

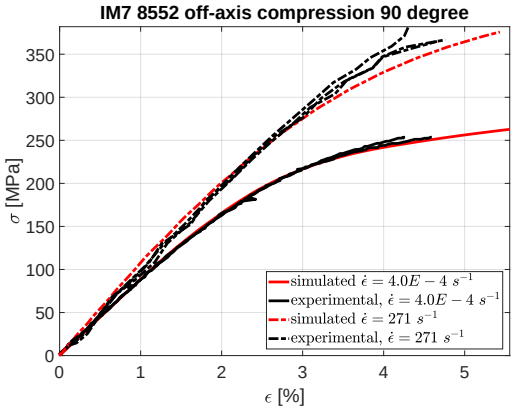

Figure 12: Axial stress-strain curves for the compression tests and simulations, 90 degree, viscoelastic-viscoplastic model.

REFERENCES

[1] H. Koerber, J. Xavier, and P. P. Camanho, "High strain rate characterisation of unidirectional carbon-epoxy IM7-8552 in transverse compression and in-plane shear using digital image correlation," *Mechanics of Materials*, vol. 42, no. 11, pp. 1004–1019, 2010.

[2] P. Kuhn, M. Ploeckl, and H. Koerber, "Experimental investigation of the failure envelope of unidirectional carbon-epoxy composite under high strain rate transverse and off-axis tensile loading," *EPJ Web of Conferences*, vol. 94, p. 01040, 2015.

[3] M. Vogler, R. Rolfes, and P. P. Camanho, "Modeling the inelastic deformation and fracture of polymer composites-Part I: Plasticity model," *Mechanics of Materials*, vol. 59, pp. 50–64, 2013.

[4] M. Kaliske and H. Rothert, "Formulation and implementation of three-dimensional viscoelasticity at small and finite strains," *Computational Mechanics*, vol. 19, no. 3, pp. 228–239, 1997.

[5] H. Poon and M. F. Ahmad, "A material point time integration procedure for anisotropic, thermo rheologically simple, viscoelastic solids," *Computational Mechanics*, vol. 21, no. 3, pp. 236–242, 1998.

[6] J. D. Schaefer, B. T. Werner, and I. M. Daniel, "Strain-Rate-Dependent Failure of a Toughened Matrix Composite," *Experimental Mechanics*, vol. 54, no. 6, pp. 1111–1120, 2014.

[7] M. Vogler, *Anisotropic Material Models for Fiber Reinforced Polymeres*. PhD thesis, Leibniz Universität Hannover, 2012.

[8] M. Vogler, H. Koerber, P. Kuhn, R. Rolfes, and P. P. Camanho, "Constitutive Modeling and Experimental Characterization of the Non-Linear Stress-Strain Behavior of Unidirectional Carbon-Epoxy Under High," *20th International Conference on Composite Materials*, 2015.